

Bonding in *cis*- and *trans*-dichlorobis(dimethylsulfide)platinum(II) studied by vibrational (micro)spectroscopy and force field calculations

M. Glerup ^{a,b}, G.O. Sørensen ^a, P. Beichert ^c, M.S. Johnson ^{a,*}

^a Department of Chemistry (KLV), University of Copenhagen, Universitetsparken 5, DK-2100, Copenhagen Ø, Denmark

^b Materials Research Department, Riso National Laboratory, Frederiksborgvej 399, 4000 Roskilde, Denmark

^c Alfred Wegener Institute for Polar and Marine Research, Am Handelshafen 12, D-27570 Bremerhaven, Germany

Received 3 March 2001; received in revised form 23 April 2001; accepted 30 April 2001

Abstract

The vibrational spectra of the square-planar complexes *cis*- and *trans*-dichlorobis(dimethylsulfide)platinum(II) have been investigated using Raman and synchrotron infrared microscopy of small samples, and mid- to far-infrared spectroscopy of macroscopic samples. Synthesis of the compounds produces the *cis*- and *trans*-stereoisomers. Using microscopy we were able to identify single crystals of the *trans* isomer and amorphous regions containing both *cis* and *trans* isomers. The infrared and Raman data are interpreted using force field calculations. Spectral shifts are discussed in terms of influence of the *cis*- and *trans*-ligands. It is found that vibrational spectroscopy is a sensitive technique for measuring subtle chemical effects in transition metal complexes which complements and may improve studies made with X-ray crystallography. © 2002 Elsevier Science B.V. All rights reserved.

Keywords: Synchrotron infrared microscopy; Raman microscopy; Platinum(II) complexes; Valence force field calculation

1. Introduction

The principal oxidation states of Pt are II and IV. The first forms square planar (and occasionally five-coordinate) complexes through five-coordinate transition states, and the latter six-coordinate complexes [1]. *Cis*–*trans* isomerism in the square planar complexes is known, given suit-

able ligands. In these systems the strength of a given metal atom–ligand bond is influenced by the ligands in the *cis* and *trans* positions. This is known as the *cis* or *trans* influence and is related to the *cis* and *trans* effect on the rate of substitution at a given site in the complex [1]. Measures of bond strength such as bond length or vibrational frequency are often used to characterize the ligand influence. A systematic series of transition metal complexes has been characterized using X-ray crystallography [2], including *cis*-dichlorobis(dimethylsulfide)platinum(II) [3] and *trans*-dichloro-

* Corresponding author. Tel.: +45-353-20303; fax: +45-353-50609.

E-mail address: msj@kiku.dk (M.S. Johnson).

bis(dimethylsulfide)platinum(II) [4,5]. Although X-ray crystallography is a straightforward way to approach the subject, the changes in geometry can be similar to the uncertainties involved in the method, due to thermal motion, experimental errors and packing effects. In contrast, vibrational spectroscopy can be a more sensitive and accurate measure of subtle effects on a given bond, and the results of the present work indicate that it can be successfully applied to these systems. While NMR, Raman and infrared spectroscopy have been used to investigate the ligand influence [6,7], this is the first study to use Raman and infrared microscopy. A straightforward method for determining the Pearson hard/soft character of metal cations based on the force constants of the square planar MCl_4^- system has been described [8]. The force constants were optimized based on infrared and Raman data.

One problem when considering the spectroscopy of systems like the title compound is that approximately equal amounts of each stereoisomer are produced during synthesis. Microscopy is a convenient technique for directly analyzing the precipitate produced during synthesis. In the present work, we were able to measure the spectra of single crystals of the *trans* compound using microscopy, including the new technique of synchrotron infrared microscopy [9], which employed a microscope at the infrared beamline at the MAX-I electron storage ring in Lund, Sweden [10]. This technique gives a significantly enhanced signal for microscopy experiments as compared with experiments performed with a blackbody light source. Complimentary information was gathered using Raman microscopy and mid- and far-infrared spectroscopy, and the results assigned with the aid of force field calculations. A number of workers have interpreted the infrared and Raman spectra of similar inorganic complexes using normal coordinate force field analysis [11,12].

2. Experimental

The isomers of dichlorobis(dimethylsulfide)platinum(II) were prepared by the following method. About 12 ml of dimethylsulfide

(DMS) were added dropwise to a solution of 2.3 g K_2PtCl_4 in 15 ml of water. The precipitate was allowed to stand overnight at room temperature and then separated by filtration [4]. Powder and single crystal X-ray diffraction showed that this precipitate contains the two isomers *cis*- and *trans*- $Cl_2(DMS)_2$ platinum(II) [4,5]. Recrystallisation was carried out in chloroform. The X-ray diffraction work showed that while both isomers can be recrystallised from chloroform, the *cis* crystals form with one molecule of chloroform which is lost when the crystals are dried, resulting in an amorphous or powdery sample. Below we present results which are consistent with single pure *trans* crystals and amorphous regions which may be *cis* or a mixture of *cis* and *trans*.

Near infrared Fourier transform (NIR-FT) Raman spectra were recorded on a Bruker model IFS 66 spectrometer equipped with a FRA 106 FT-Raman module connected via optical fibers to a Bruker RamanmicroscopeTM. The light source was a Nd:YAG laser with an excitation wavelength of 1064 nm. The spectrometer was equipped with a Ge-detector cooled to liquid nitrogen temperature. The Raman shift cut-off at high frequency is 3500 cm^{-1} , and a narrow band frequency filter removes the spectral features in the region from 84 to -100 cm^{-1} . A $40\times$ objective was used in the microscope, giving an approximate spot size diameter of $30\text{ }\mu\text{m}$. The spectral resolution was around 6 cm^{-1} for the apodized spectra. All spectra have been post zero-filled with a factor of eight. The spectra were measured on nominally perfect crystals, and on amorphous areas in the sample.

A Bruker infrared microscope was used in combination with the Bruker IFS 120 HR interferometer at the beamline for infrared spectroscopy at the MAX-I electron storage ring at MAX-Lab in Lund, Sweden. The facilities have been described earlier [10,13], and only the part necessary for an understanding of this experiment is described here. The microscope was equipped with an MCT detector, a NaCl beamsplitter and a Cassegranian telescope geometry. Experiments could be performed either in transmission or reflection at approximately normal incidence. The interferometer beam entered the microscope housing via a 25

mm diameter KBr window. By combining the field lens (15 or 36 \times magnification) with the 20 \times ocular, magnifications of 300 and 720 were realized. Using the smallest microscope aperture of 0.3 mm the spatial resolution is nominally 8 μm . At this resolution, given the microscope's numerical aperture of 0.5, far field microscopy is diffraction limited for frequencies less than about 1500 cm^{-1} . At 1000 cm^{-1} the resolution is limited by diffraction for spatial resolutions less than 12 μm . In reflection mode the NaCl beamsplitter prevents use of the microscope below 700 cm^{-1} , a limit similar to that due to the MCT detector. A video camera was used to locate single crystals or amorphous regions of the sample which was placed on a first surface mirror.

The far infrared (FIR) Fourier transformed spectrum, 100–600 cm^{-1} , has been measured on a Bruker IFS120 HR with a Globar lamp as the light source and equipped with a deuterium triglycine sulfate (DTGS) detector working at room temperature. A 3.5 μm Mylar beam splitter was used. The interferogram was zero filled with a factor of two and no apodization was used. The spectrum was obtained with 32 scans and a spectral resolution of 2 cm^{-1} . Two mg of sample and 200 mg of polyethylene were pressed in standard KBr press.

The mid infrared (MIR) spectrum, 400–3500 cm^{-1} , has been measured on a Perkin Elmer 1760X spectrometer equipped with a DTGS detector. Three mg of the *cis-trans* complex were pressed into a tablet in 200 mg of potassium bromide. The spectrum was obtained with 32 scans and spectral resolution of 2 cm^{-1} .

3. Theoretical

The vibrational spectrum was calculated using the Wilson FG matrix method [14]. The compounds have 57 normal modes. For the *cis* configuration the symmetry group is C_1 (i.e. no symmetry); IR and Raman transitions are allowed for all normal modes. The *trans* isomer (symmetry group C_{2h}) has an inversion center. For groups with such a center the rule of mutual exclusion states that a given normal mode can be either IR

or Raman active but not both; species A_u and B_u are IR active and A_g and B_g Raman active.

Calculations are based on the transfer of structural data and force constants from the building blocks, the PtCl_4^{2-} ion and the dimethyl sulfide molecule, found in the literature. This procedure was followed in a study of the corresponding *trans* palladium complex [15] and our calculations are performed in a similar way. The program VIBROT was used for the calculations. Documentation and source code in C written for UNIX-like platforms is available by ftp [16] together with the input files for the present calculations.

3.1. PtCl_4^{2-} ions

Force constant calculations for this ion were described by Jones [17], and later reinvestigated by Goggin et al. [18]. The ion has D_{4h} symmetry with a Pt–Cl bond length of 1.33 Å. The mean atomic weight of Pt, 195.08 U, was used.

The redundancy among the four Cl–Pt–Cl internal bending coordinates can be eliminated in the symmetry coordinates. The four out of plane coordinates are defined following Wilson, Decius and Cross [14] as $\text{Cl}_i\text{Cl}_j\text{Pt}-\text{Cl}_k$ with cyclic combination of i, j, k from the cyclic atomic numbering of the Cl atoms. They include two redundancies that can be removed in forming the symmetry coordinates. Alternatively, the calculations can be performed directly using the valence coordinates, since the VIBROT program incorporates a procedure for the automatic removal of redundancies described by Sørensen [19]. The force constants and frequencies are given in Table 1. The number of digits given for the force constants does not reflect their uncertainty, but are included to ensure that our calculations can be reproduced. The frequencies reproduce the assignment of Jones [17].

3.2. Dimethyl sulfide ions

Our calculations were based on the work by Tranquille et al. [20]. For the structure with C_{2v} symmetry we have used C–H distances 1.093 Å,

Table 1
Force constants and calculated frequencies for $[\text{PtCl}_4]^{2-}$

Vibration	Force constant ^a	Symmetry and calculated frequencies, cm^{-1}
$\tilde{\nu}(\text{PtCl})$	1.772243	A_{1g} : 328
$\tilde{\nu}(\text{PtCl}, \text{PtCl}')$	0.074990	B_{1g} : 305
$\tilde{\nu}(\text{PtCl}, \text{PtCl}'')^b$	0.294338	B_{2g} : 173
$\tilde{\nu}(\text{ClPtCl}')$	1.215976	A_{2u} : 147
$\tilde{\nu}(\text{PtCl}, \text{ClPtCl}'')$	0.060000	B_{2u} : 112
$\tilde{\nu}(\text{ClPtCl}', \text{Cl}'\text{PtCl}'')$	0.189535	E_g : 313, 165
$\tilde{\nu}(\text{outo})$	0.351920	—

^a Units are $\text{mdyn per } \text{\AA}$, $\text{mdyn}\text{\AA per rad}^2$ and mdyn per rad , $\text{mdyn} = 10^{-8} \text{ N}$.

^b $\text{Cl-Pt-Cl}''$ colinear.

Table 2
Force constants and calculated frequencies for DMS

Mode	Force Constant ^a	Symmetry and Calculated Frequencies, cm^{-1}
$\tilde{\nu}(\text{CHp})$	4.833425	A_1 : 2997, 2928, 1446, 1339, 1038, 695, 278
$\tilde{\nu}(\text{CHo})$	4.762826	
$\tilde{\nu}(\text{CH}, \text{CH}')$	0.049455	
$\tilde{\nu}(\text{CS})$	3.258269	
$\tilde{\nu}(\text{CS}, \text{CS}')$	−0.089515	A_2 : 2979, 1438, 949, 162
$\tilde{\nu}(\text{SCHp})$	0.489094	
$\tilde{\nu}(\text{SCHo})$	0.706632	
$\tilde{\nu}(\text{SCHo}, \text{SCH}''\text{o})$	0.067889	
$\tilde{\nu}(\text{SCHp}, \text{SCHo})$	−0.103401	B_1 : 2995, 2928, 1438, 1312, 899, 740
$\tilde{\nu}(\text{SCHp}, \text{SCH}''\text{p})$	0.100757	
$\tilde{\nu}(\text{SCHo}, \text{SCH}''\text{o})$	0.005842	
$\tilde{\nu}(\text{HCHp})$	0.503122	
$\tilde{\nu}(\text{HCHO})$	0.523348	B_2 : 2979, 1440, 972, 170
$\tilde{\nu}(\text{CSC})$	0.949485	
$\tilde{\nu}(\text{CH}, \text{CS})$	−0.344100	
$\tilde{\nu}(\text{CS}, \text{SCHp})$	0.280018	
$\tilde{\nu}(\text{CS}, \text{SCHo})$	0.302584	
$\tilde{\nu}(\text{CH}, \text{SCH})$	−0.038552	
$\tilde{\nu}(\text{tors: CSCH})$	0.015856	

^a Units are $\text{mdyn per } \text{\AA}$, $\text{mdyn}\text{\AA per rad}^2$ and mdyn per rad .

CS distances of 1.802 \AA , tetrahedral angles for the methyl groups and a CSC angle of 98.90°. For the hydrogens in the CSC-plane the HCSC chains have a *trans* configuration.

The force constants obtained by the VIBROT program shown in Table 2 resulted from a fit to the observed frequencies of DMS, $\text{D}_3\text{-DMS}$ and $\text{D}_6\text{-DMS}$ given in [20]. Using the approach of Tranquille et al. [20], the CH_3 -groups were treated in a lower symmetry than C_{3v} . A distinction is made by the subscript p or o; a p-force constant involves an internal coordinate that is symmetric with respect to the plane of the CSC atoms. The subscript o refers to the corresponding pair of anti-symmetrized internal coordinates. Atoms H and H' belong to different methyl groups in equivalent positions.

3.3. The *trans* complex

The *trans* complex has C_{2h} symmetry. This structure is similar to the corresponding Pd complex [15] as shown by a recent X-ray investigation [5]. Drawings of the structure of the *cis* and *trans* complexes are given in Fig. 1, based on the X-ray study. To within the uncertainties of that work, the structure of DMS is very similar in the Pt and Pd complexes. This means that the CSC planes of the two DMS ligands are perpendicular to the plane of PtCl_2S_2 . The Pt–Cl and Pt–S distances were found to be 2.297 and 2.309 \AA , respectively, and for the Pt–S–C angles we have used the value 106.8° that is the average value for the four Pt–S–C angles. Finally the Cl–Pt–S angles were set to 92.4 and 87.6° in such a way that the Cl–C distances are slightly changed from the values for 90° angles.

Most of the force constants were transferred unchanged from the values found for the Pd-complex [15]. In Table 3 we show the changes and additions we have introduced in order to fit the lower frequencies of the Pt-core as compared with the Pd-compound. Observed and calculated Raman frequencies are given in Table 4; all the calculated IR and Raman frequencies given in Table 5 and Table 6.

3.4. The *cis* complex

An X-ray investigation of the structure of the

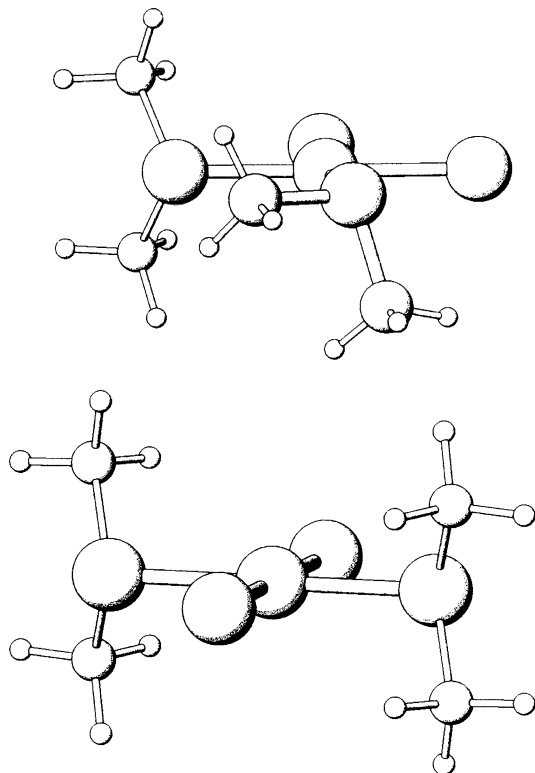


Fig. 1. Geometries of the *cis* and *trans* isomers [5].

cis complex has been presented by Horn et al. [3]. The symmetry is C_1 with the PtCl_2S_2 almost situated in a plane. For one of the DMS molecules the SCS plane is almost perpendicular to the

PtCl_2S_2 ‘plane’ whereas the other DMS molecule has one of the S atoms nearly in the PtCl_2S_2 ‘plane’. We have used the structural parameters determined by the X-ray investigation [3]. In the first attempt, the valence force constants of the *trans* complex were transferred without any changes. This gave rise to a Pt–Cl band placed at 375 cm^{-1} . Vibrations from bonds between electron rich atoms have a high polarisability and are typically intense in a Raman spectrum. No bands are observed in the Raman spectrum at wavenumbers higher than 360 cm^{-1} , therefore, two force constants were modified to decrease the vibrational frequency of the Pt–Cl symmetrical stretch band. The $f(\text{Pt–Cl})$ force constant was decreased to 1.8 mdyn per Å which is nearly the initial value of the $f(\text{Pt–Cl})$ force constant in the PtCl_4^{2-} ion. The interaction force constants $f(\text{PtCl, PtS})$, $f(\text{PtCl, PtCl})$, $f(\text{PtS, PtS})$ were increased to 0.13 mdyn per rad , giving a lower frequency for the Pt–Cl symmetrical stretch vibration; all calculated frequencies are given in Table 6.

4. Results and discussion

A far infrared spectrum was recorded for a mixture of the complexes in a polyethylene pellet. Results are shown for the frequency region $100\text{--}800\text{ cm}^{-1}$ in Fig. 2, together with two different

Table 3

Force constants fitted for the A_g and B_g frequencies of the *trans* complex^a

Mode	Specie	Initial value	Final value
$f(\text{PtCl})$	(PtCl_4)	1.772243	2.044776
$f(\text{PtS})$	–	–	1.520539
$f(\text{PtCl, PtS})$	–	–	0.074990
$f(\text{PtS, PtS}) = f(\text{PtCl, PtCl})$	(PtCl_4)	0.294338	0.294338
$f(\text{ClPtS})$	(PtCl_4)	1.215976	1.864919
$f(\text{ClPtS, SPtCl}) = f(\text{ClPtS, S'PtCl})$	(PtCl_4)	0.189535	0.189535
$f(\text{CS})$	(DMS)	3.258269	3.074018
$f(\text{CSC})$	(DMS)	0.949485	1.044587
$f(\text{ClPtSC})$	–	–	0.012000
$f(\text{outo})$	(PtCl_4)	0.351920	0.351920

^a Units are mdyn per Å , mdynÅ per rad^2 and mdyn per rad .

Table 4
Raman frequencies in cm^{-1} for the *trans* complex^a

Assignment	Observed	Calculated	Observed – Calculated
<i>A_g</i>			
CHa	2999	2997.3	–
CHa	?	2979.5	–
CHs	2919	2927.7	–
HCHa	1419	1446.4	–
HCHa	?	1440.3	–
SCHs	1322	1338.4	–
SCHa	1032	1038.9	–
SCHa	989	978.8	–
CSs	683.1 ^b	684.3	–1.2
PtSs	344.0 ^b	346.1	–2.1
PtCls	329.9 ^b	327.8	2.1
CSC	295.9 ^b	296.4	–0.5
ClPtS	204.1 ^b	204.2	–0.1
CH ₃ (tors)	169.6 ^b	169.5	0.1
PtSC	?	139.6	–
<i>B_g</i>			
Cha	2999	2995.4	–
Cha	?	2979.4	–
CHs	2919	2927.9	–
HCHa	1419	1438.7	–
HCHa	?	1437.9	–
SCHs	1322	1311.0	–
SCHa	951	951.6	–
SCHa	?	900.1	–
Csa	724.8 ^b	723.6	1.2
PtSC	204.1 ^b	205.8	–1.7
CH ₃ (tors)	?	154.8	–
Pt-SCC(tors)	?	26.8	–

^a The difference between the observed and the calculated vibrational frequency is given in the fourth column for the vibrations used to optimize the fit.

^b Included in the fit.

Raman microscopy spectra. The Raman spectra were recorded on an amorphous region of the sample, and on a single crystal. Force field calculations only predict significant differences for frequencies below 400 cm^{-1} (Tables 5 and 6), in accordance with the experimental observations.

In Fig. 2 more bands are seen in the solid curve than in the dotted curve. The lower symmetry of the *cis* compound results in more allowed vibrational transitions, leading us to the conclusion that the single crystal is the *trans* isomer (dotted spectrum). The amorphous region most likely consists of a mixture of the *cis* and *trans* complexes since

the *trans* peaks observed in the dotted spectrum are also observed in the solid spectrum, c.f. Fig. 2.

The force field calculation verifies the above statement. The Pt-S-Cl vibration (237.7 cm^{-1}) is only IR allowed whereas the same vibration for the *cis* compound (235.5 cm^{-1}) is IR and Raman active. In the Raman spectrum (c.f. Fig. 2) we do not observe any bands at approximately 235 cm^{-1} for the *trans* compound (dotted spectrum) but the spectrum measured on the amorphous region (solid spectrum) contains a band at 235 cm^{-1} . The IR spectrum also contains a strong vibrational band at 235 cm^{-1} , corresponding to the sum of the Pt-S-C band from the *cis* and *trans* complex. The force field calculation predicts that the *trans* compound (dotted spectrum) should not have any active Raman vibrations in the frequency region $296\text{--}318\text{ cm}^{-1}$ whereas the *cis* compound should have one allowed Raman transition, in accordance with the experimental results.

The Raman spectrum of the *trans* compound was measured on samples with different crystal orientations. The main difference is the intensity ratios between the peaks placed at 683 and 725 cm^{-1} and the peaks placed at 330 cm^{-1} and 343 cm^{-1} . This is expected since the laser light is slightly polarized and the crystal orientation changes from one experiment to the next.

Fig. 3 shows the MIR spectrum for the *cis* and *trans* isomers measured using a KBr pellet. A Raman spectrum is shown in Fig. 3 as a reference; all the Raman spectra are alike in this frequency region, in accordance with the force field calculations; e.g. Tables 5 and 6.

The spatial resolution of the IR-synchrotron microscopy experiment was higher than in the Raman experiment, but the frequency range was limited to the medium infrared region above 700 cm^{-1} by the beamsplitter and detector in the microscope. The force field calculations indicate that the *cis* and *trans* isomers have very similar spectra (Tables 5 and 6) in this frequency region. The single crystals were seen to have large flat faces following recrystallization; their size was from 2 to 60 microns measured using a video camera attached to the infrared microscope. Spectra were measured of single crystals and amor-

phous regions, and variations are seen from one sample to the next as shown in Fig. 4.

In Fig. 4a, the CH stretching band of the dimethyl sulfide ligand is displayed. The contour

of this band changes depending on the crystal. The changes are similar to those observed in *cis*- and *trans*-Pt(II) bis(glycino) complexes [21]. The synchrotron is a polarized light source (75% in the

Table 5

Compilation of vibrational frequencies obtained from the force field calculation for *trans*-Pt(DMS)₂Cl₂

<i>trans</i> -Pt(DMS) ₂ Cl ₂							
A _u		B _u		A _g		B _g	
IR		IR		Raman		Raman	
CHa	2997.3	CHa	2995.4	CHa	2997.3	CHa	2995.4
CHa	2979.5	CHa	2979.4	CHa	2979.5	CHa	2979.4
CHs	2927.7	CHs	2927.9	CHs	2927.7	CHs	2927.9
HCHa	1446.4	HCHa	1438.7	HCHa	1446.4	HCHa	1438.7
HCHa	1440.3	HCHa	1437.9	HCHa	1440.3	HCHa	1437.9
SCHs	1338.4	SCHs	1311.0	SCHs	1338.4	SCHs	1311.0
SCHa	1038.8	SCHa	951.6	SCHa	1038.9	SCHa	951.6
SCHa	978.4	SCHa	900.6	SCHa	978.8	SCHa	900.1
CSs	684.1	Csa	726.9	CSs	684.3	CSa	723.6
PtCla	347.4	PtSC	227.8	PtSs	346.1	PtSC	205.8
CSC	318.5	CH ₃ (tors)	158.2	PtCls	327.8	CH ₃ (tors)	154.8
PtSC	290.6	Pt-op	132.2	CSC	296.4	Pt-SCC(tors)	26.8
PtSa	237.7	ClS-op	81.7	ClPtS	204.2	—	—
ClPtS	187.0	Pt-SCC(tors)	20.4	CH ₃ (tors)	169.5	—	—
CH ₃ (tors)	158.7	—	—	PtSC	139.6	—	—
ClPtS	112.2	—	—	—	—	—	—

Table 6

Compilation of vibrational frequencies obtained from the force field calculation for *cis*-Pt(DMS)₂Cl₂

<i>cis</i> -Pt(DMS) ₂ Cl ₂					
CHa1	2997.5	HCHa'1	1437.8	PtSCw2	322.9
CHa2	2997.4	SCHs1	1338.6	PtCla	301.3
Cha'1	2995.5	SCHs2	1338.5	CSC2	296.3
CHa'2	2995.4	SCHs'1	1311.3	CSC1	275.6
CHa'2	2979.5	SCHs'2	1311.2	PtSCr1	235.5
CHa'1	2979.5	SCHa1	1040.3	ClPtS	224.3
CHa2	2979.4	SCHa2	1039.9	PtSCr2	217.4
CHa1	2979.4	SCHa'1	979.8	PtSa	206.0
CHs'2	2927.9	SCHa'2	979.4	PtSCw1	195.2
CHs'1	2927.9	SCHa1	952.4	CH3-1(tors)	162.9
CHs1	2927.8	SCHa2	952.2	CH3'2(tors)	159.2
CHs2	2927.7	SCHa'	902.4	CHs-2(tors)	157.8
HCHa2	1446.4	SCHa'2	901.1	CH3'1(tors)	153.9
HCHa1	1446.3	CSa1	729.0	ClPtS	137.9
HCHa'2	1440.2	CSa2	726.1	Pt-op	117.2
HCHa'1	1440.2	CSs2	684.1	ClPtCl	113.5
HCHa2	1438.6	CSs1	682.9	ClS-op	95.9
HCHa1	1438.6	PtCls	351.3	Pt-SCC1(tors)	23.5
HCHa'2	1437.8	PtSs	348.7	Pt-SCC2(tors)	23.0

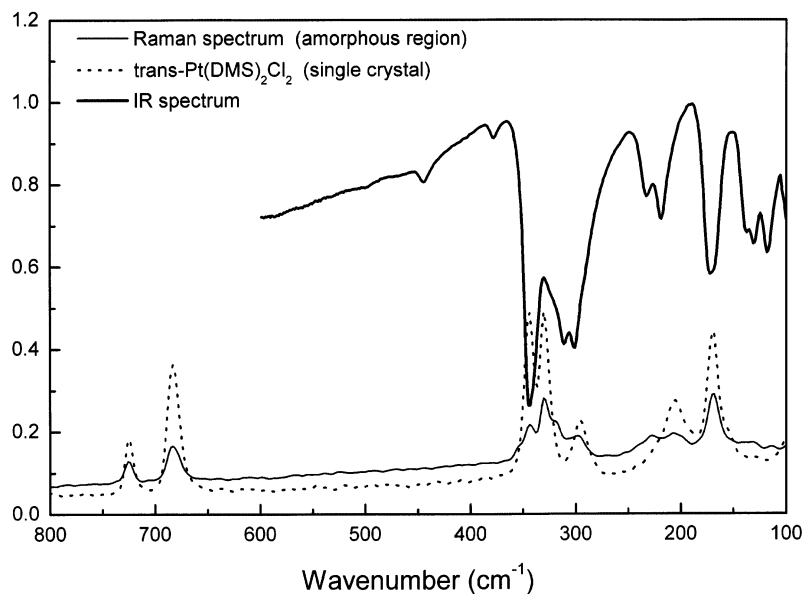


Fig. 2. FIR spectrum of the isomeric compound $\text{Pt}(\text{DMS})_2\text{Cl}_2$ pressed in polyethylene, shown as a transmittance spectrum (thick curve). The dotted curve is the NIR-FT-Raman spectrum of the *trans*- $\text{Pt}(\text{DMS})_2\text{Cl}_2$ compound (single crystal) and the thin curve is the spectrum of *cis-trans*- $\text{Pt}(\text{DMS})_2\text{Cl}_2$ (amorphous region).

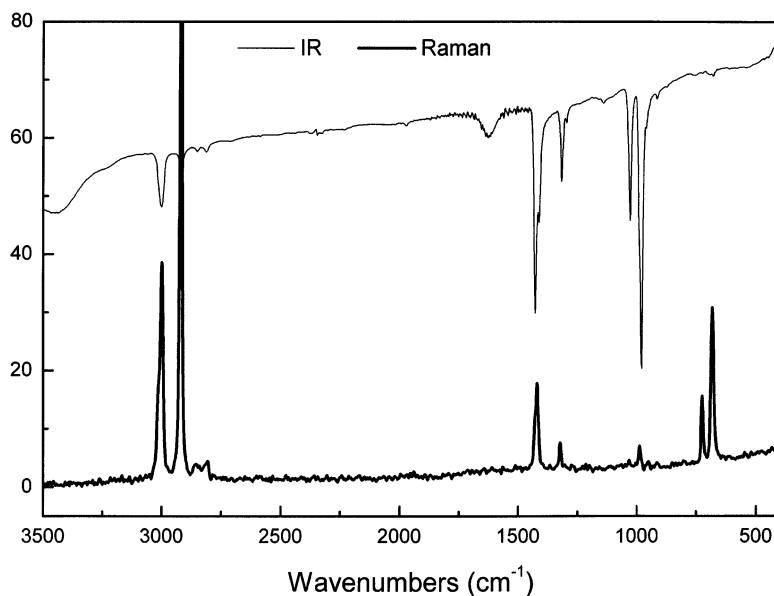


Fig. 3. The MIR transmission spectrum of *cis-trans*- $\text{Pt}(\text{DMS})_2\text{Cl}_2$ pressed as a KBr pellet, shown as a transmittance spectrum (thin curve). The thick curve is the NIR-FT-Raman spectrum; only one spectrum is shown since in this frequency region it is not possible to differentiate between the two isomers.

plane of the storage ring), and it is possible that crystal orientation may also play a role in the intensity variations seen in Fig. 2. Thus the inten-

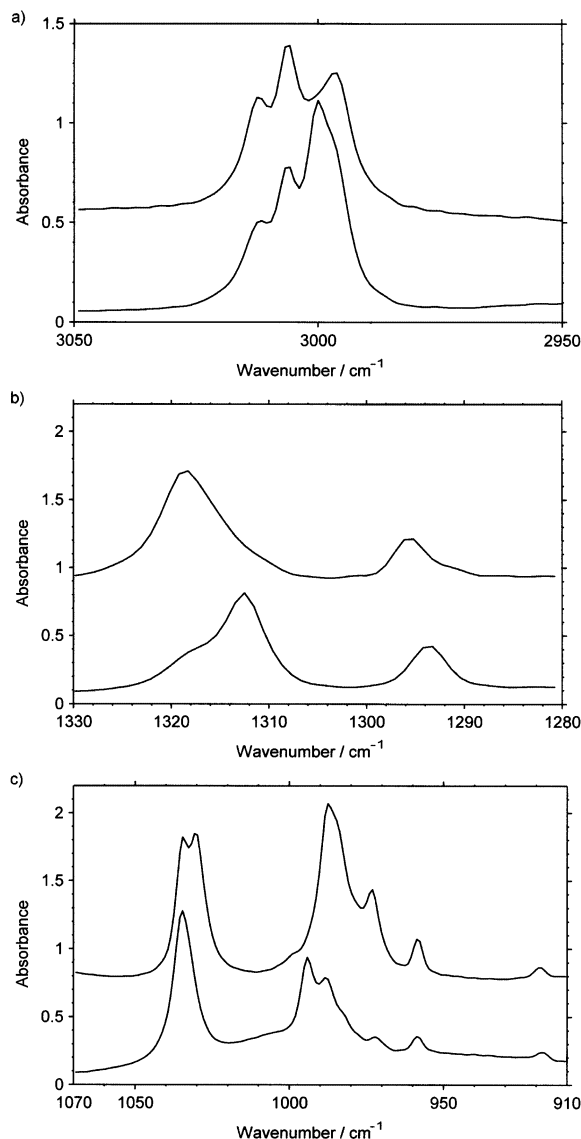


Fig. 4. Spectra of two crystals of the isomeric compound $\text{Pt}(\text{DMS})\text{Cl}_2$. The same crystal is on top in each figure. (a) displays the frequency region 2950–3050 cm^{-1} , showing how the contour of the CH stretching band of the dimethylsulfide ligand changes depending on the crystal, (b) is from 1280–1330 cm^{-1} , showing a clear change in peak location from 1313 to 1319 cm^{-1} , and from 1294 to 1296 cm^{-1} , (c) shows changes in the frequency region of 910–1070 cm^{-1} .

sity variations cannot be assigned as arising only from varying concentrations of *cis* or *trans* isomers.

Fig. 4(b) is from 1280 to 1330 cm^{-1} , showing a clear change in peak location from 1313 to 1319 cm^{-1} , and from 1294 to 1296 cm^{-1} . Fig. 4(c) shows changes in the frequency region of 910–1070 cm^{-1} . The force field fitting process was based on the low frequency bands (Table 4), therefore, the possibility of assigning bands in the mid infrared region is limited.

It is remarkable that the frequency of the CH stretching vibrations 2919 and 2999 cm^{-1} , shown in Figs. 3 and 4 and Tables 4–6 are high compared with the typical sp^3 CH stretching frequency. We cannot give a fundamental explanation for the band position changes in the infrared microscopy spectra. The bands are not due to artifacts since they are also observed in the MIR spectrum of the sample measured as a powder.

Despite the analysis of many samples and repeated searches, pure *cis* crystals were not observed in our experiment. Perhaps the *trans* compound forms crystals more readily due to the effect of the center of inversion on its charge distribution.

5. Conclusion

The Raman data show that the low frequency region of the spectrum is especially useful for assigning the vibrational modes of transition metal complexes, since this is the spectral region corresponding to ligand-metal vibration. At the beam-line for infrared microscopy being planned for the MAX-III storage ring, currently under construction in Lund Sweden, we will have the special detectors and a modified microscope for investigating this key spectral region. As opposed to black-body light sources, the intensity of light from the storage ring increases with decreasing wavenumber, presenting a significant advantage for diffraction limited microscopy, even at wavelengths/diffraction limited spot sizes extending through the far infrared to the millimeter wave region. This will give us the opportunity to expand this study and make more direct correlations to the low frequency Raman spectra.

In this study we were able to distinguish between the *cis* and the *trans* isomers due to symmetry, and because of the force field calculation we could verify our initial conclusion and assign some of the vibrational bands.

X-ray crystallography can resolve bond lengths to less than 1 in 10^2 , while vibrational spectroscopy resolves frequency to 1 in 10^3 or 10^4 . It is worthwhile to compare these two techniques in their ability to examine subtle bonding effects.

With reference to Fig. 1, we can now analyze the *cis* and *trans* ligand influence. In the *cis* compound the Pt–Cl bond is *trans* to DMS and *cis* to both Cl^- and DMS. In the *trans* compound the same bond is *trans* to Cl^- and *cis* to two DMS molecules. The fact that we had to lower the force constant for the Pt–Cl stretch vibration for the *cis* compound to get a better match to the observed data implies that the Cl^- ion is more strongly bound in the *trans* complex. Since it is known that the *cis* influence has little effect on the Pt–Cl bond length, the results suggest that the *trans* influence of chloride is higher than that of DMS. Evaluating the *trans* influence using the magnitude of the force constants has been discussed by T.G. Appleton et al. and L.I. Elding et al. [6,7]. The present work confirms that it is a valuable tool.

An analysis of the geometry of 22 Pt(II) complexes obtained by X-ray crystallography was not able to differentiate between the *trans* effect of DMS and Cl^- since the differences in bond length (1% of a bond distance of ca 2.3 Å) are comparable to the errors inherent to the technique. The techniques used in this paper are able to identify the particular eigen-frequency involved with a given vibration and although more work is necessary, the results show that vibrational spectroscopy is inherently a sensitive indicator of subtle variations in the chemical bonding of these systems.

The work of Løvqvist and Giveen in the group of Oskarsson [2,5] indicates that the *cis* influence is more important for Pt–S bonds than Pt–Cl bonds. From X-ray crystallography it is known that sulfur has a greater *cis* influence on the Pt–S bond than chloride, and that S also has a greater *trans* influence on the Pt–S bond than chlorine. Since the DMS ligand has a *cis* Cl^- in each

isomer, we can conclude that a *cis* DMS influence plus a *trans* Cl^- influence has about the same effect as a *cis* Cl^- plus a *trans* DMS. This is consistent with the result of the X-ray studies indicating that DMS has both a greater *cis* and a greater *trans* influence on the Pt–S bond than Cl^- .

Acknowledgements

One of the authors (M. Glerup) would like to thank the Danish Research Academy for general funding. The authors are grateful to Haldor Topsøe A/S and to the Danish Natural Research Council for funding the NIR-FT-Raman instrument within the material science program. The authors would like to thank Åke Oskarsson of the Inorganic Chemistry Department, Lund University for synthesizing the compounds used in this study. Daniel Christensen of the Department of Chemistry, University of Copenhagen provided valuable assistance with recording the Raman and infrared spectra. The experiments would not have been possible without the assistance of Bengt Nelander and the staff of the MAX-Lab storage ring in Lund Sweden. In addition, we gratefully acknowledge Professor Otto Schrems of the Alfred Wegener Institute in Bremerhaven Germany for lending us an infrared microscope, and Ole Faurskov Nielsen of the University of Copenhagen for valuable discussions.

References

- [1] F.A. Cotton, G. Wilkinson, Advanced Inorganic Chemistry, Fifth ed., Wiley, New York, 1988.
- [2] K. Løvqvist, A Crystallographic Study of Platinum(II) Complexes, Ph.D. Thesis, University of Lund, Sweden, 1996, and references therein.
- [3] G.W. Horn, R. Kumar, A.W. Maverick, F.R. Fronczek, S.F. Watkins, Acta Cryst. C46 (1990) 135.
- [4] E.G. Cox, H. Saenger and W. Wardlaw, J. Chem. Soc. (1934) 182.
- [5] D. Giveen, Packing characteristics of centrosymmetric Pt- and Pd- complexes; The crystal structures of *trans*-dichlorobis(dimethylsulfide) platinum(II) and *trans*-dichlorobis(methylphenylsulfide) palladium(II), M.Sc. Thesis, University of Lund, Sweden, 2000.

- [6] T.G. Appleton, H.C. Clark, L.E. Manzer, *Coord. Chem. Rev.* 10 (1973) 335.
- [7] L.I. Elding, Ö. Gröning, *Inorg. Chem.* 17 (1978) 1872.
- [8] H.O. Desseyn, S.P. Perlepes, A.C. Fabretti, *App. Spect.* 45 (1991) 131.
- [9] G.P. Williams, P. Dumas, *Infrared Microspectroscopy with Synchrotron Radiation, Accelerator-Based Infrared Sources and Applications*, Proceedings of SPIE 3153, 1997.
- [10] M.S. Johnson, P. Beichert, O. Schrems, B. Nelander, *Asian Chem. Lett.* 4 (2000) 45.
- [11] T.R. Cundari, W. Fu, E.W. Moody, L.L. Slavin, L.A. Snyder, S.O. Sommerer, T.R. Klinckman, *J. Phys. Chem.* 100 (46) (1996) 18057.
- [12] L. Chong-De, L.-J. Jiang, W.-X. Tang, *Spectrochim. Acta* 49A (3) (1993) 339.
- [13] M.S. Johnson, B. Nelander, *Il Nuovo Cimento* 20D (1998) 449.
- [14] E.B. Wilson, J.C. Decius, P.C. Cross, *Molecular Vibrations*, McGraw Hill, New York, 1955.
- [15] M. Tranquille, M.T. Forel, *J. Mol. Struct.* 25 (1974) 413.
- [16] G.O. Sørensen, anonymous@kl5axp.ki.ku.dk, 2001.
- [17] L.H. Jones, *Coord. Chem. Rev.* 1 (1966) 351.
- [18] P.L. Goggin, J. Mink, *J. Chem. Soc. (Dalton)* (1974) 1479.
- [19] G.O. Sørensen, *J. Mol. Spec.* 35 (1970) 489.
- [20] M. Tranquille, P. Labarbe, M. Fouassier, M.T. Forel, *J. Mol. Struct.* 8 (1971) 273.
- [21] K. Nakamoto, *Infrared and Raman Spectra of Inorganic and Coordination Compounds*, Fourth ed., Wiley, New York, 1986, p. 235.